OFFICE OF NAVAL RESEARCH

CONTRACT N00014-87-K-0109

87 MAR 01 - 88 FEB 28

S400007SRR

FIRST ANNUAL TECHNICAL REPORT

413 - IR REFLECTANCE AND RAMAN SCATTERING

OF DIAMOND FILMS

by

George E. Walrafen

Chemistry Department

Howard University

500 College St., N. W.

Washington, D. C. 20059

Office (202) - 636-6897 or 6564

Home (202) - 362-9430

DD Form 1473

1a. UNCLAS

1b. none

3. Approved for public release; distribution unlimited

5. S400007SRR

7a. ONR-1114

7b. Arlington, VA 22217

8a. SDIO/IST

8b. Pentagon, Washington, DC 20301-7100

10a. PE 63220

10b. I.S.T.

10c. 6.2

10d. S400007SRR

20. UNCLAS/UNLIMITED

21. UNCLAS

other items are self-explanatory and are to be completed prior to report distribution.

Accession For	
NTIS GRA&I	☑
DTIC TAB	☐
Unannounced	☐
Justification	
By	
Distribution/	
Availability Codes	
Dist	Avail and/or Special
A-1	

413 - IR REFLECTANCE AND RAMAN SCATTERING OF DIAMOND FILMS

-Outline-

1. Nature of Work.
   - A. Service work for other SDIO/IST contractors.
   - B. Investigative Work.
2. Results.
   - A. Raman spectra from diamond films.
   - B. Raman spectra from diamond and graphite.
   - C. Raman spectra from a wide range of amorphous carbons.
3. Interpretation.
   - A. The narrow 1330 cm^{-1} and the ca. 1600 cm^{-1} features from diamond films.
   - B. Evidence bearing on the width of the broad 1350 cm^{-1} feature; possible relation to diamond growth.

1. Nature of work.

A. Service work for other SDIO/IST contractors.

A significant amount of the first years work on this contract (ca. 50%) involved service work to characterize and evaluate diamond films supplied by other SDIO/IST contractors. (We include in this category, service work for participants at the past two diamond film meetings, some of whom may be prospective SDIO/IST contractors, e.g., Flamm at Bell Laboratories, Machonkin at Xerox, Rabalais at the University of Houston, Steiger at PPG, etc.) Some of the SDIO/IST contractors for whom we did service work are: Markunas and Rudder at RTI, and Pinneo at Crystallume. We expect to receive samples from Geis at MIT very soon. These MIT samples involve diamond grown epitaxially on a diamond substrate.

B. Investigative work.

The investigative work has involved analysis and interpretation of the features seen from the diamond films supplied by various workers mentioned in A, above.

From the various diamond films, three general types of peaks were seen. These correspond to peak frequencies of 1330/cm^{-1} (a very sharp peak), ca. 1350/cm^{-1} (a very broad peak), and ca. 1600/cm^{-1} (a broad and sometimes structured contour). To understand these three classes of peaks we obtained Raman spectra from bulk crystalline diamond, from various graphites, and from a wide range of amorphous carbons. The data and tentative interpretation are presented below.

2. Results.

A. Raman spectra from diamond films.

In this category we will present Raman spectra from three general types of diamond films: (i) Raman spectra from films which contain no crystalline diamond, but which display the broad 1350 cm^{-1} and 1600 cm^{-1} features, (j) Raman spectra from films with some crystalline diamond, and hence that show the very sharp 1330 cm^{-1} peak, plus the broad 1350 and 1600 cm^{-1} features, and (k) Raman spectra from diamond films that are almost entirely composed of crystalline diamond, and which show an extremely intense 1330 cm^{-1} peak. Evidence for the assignment of the sharp 1330 cm^{-1} peak to crystalline diamond, and for the assignment of the broad 1600 cm^{-1} feature is presented in section 2b, below.

(i) Figs. 1 and 2 refer to films that contain no crystalline diamond. The Raman spectra from these films only show the broad 1350 and 1600 cm^{-1} peaks.

(j) Figs. 3 and 4 refer to films that contain some crystalline diamond. Here the sharp 1330 cm^{-1} crystalline diamond peak is superimposed on the contour formed by the broad 1350 and 1600 cm^{-1} features.

(k) Fig. 5 refers to the Raman spectrum from a diamond film that is composed predominantly of diamond twins over its entire surface. Here, the contour containing the broad 1350 and 1600 cm^{-1} features is extremely weak--note that the concavity is upward from about 1000 to 1300 cm^{-1}, whereas the concavity is <u>downward</u> from about 1400 to 1700 cm^{-1} because of these two features. The sharp 1330 cm^{-1} feature is very intense.

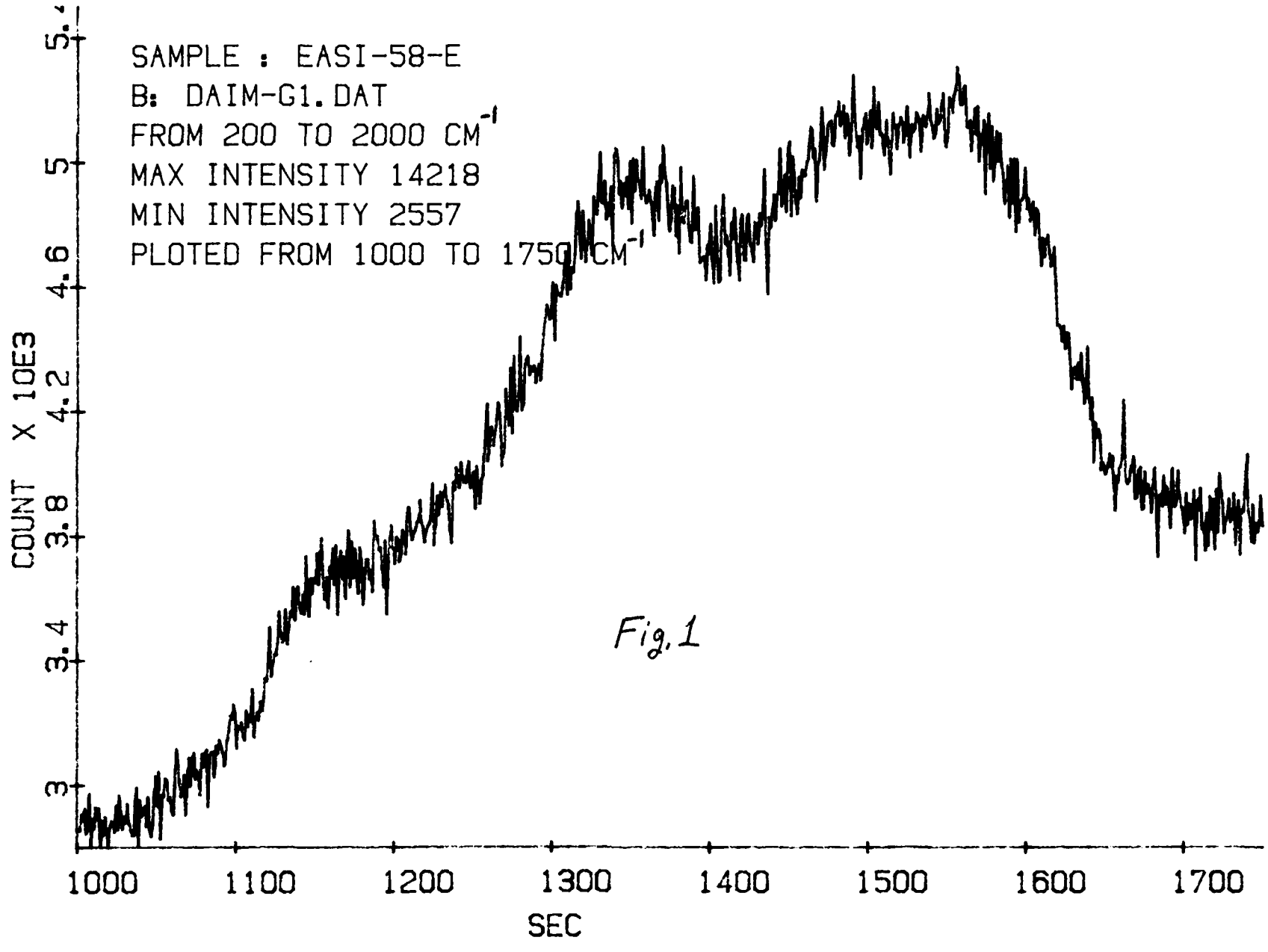

Fig. 1

LASER: 500 MW @ 514.5 NM. SLITS: 10 MIC. DATE 05-21-87

1 SCAN(S), TIME: .6 SEC/PT, PTS SPACED BY 1 SEC

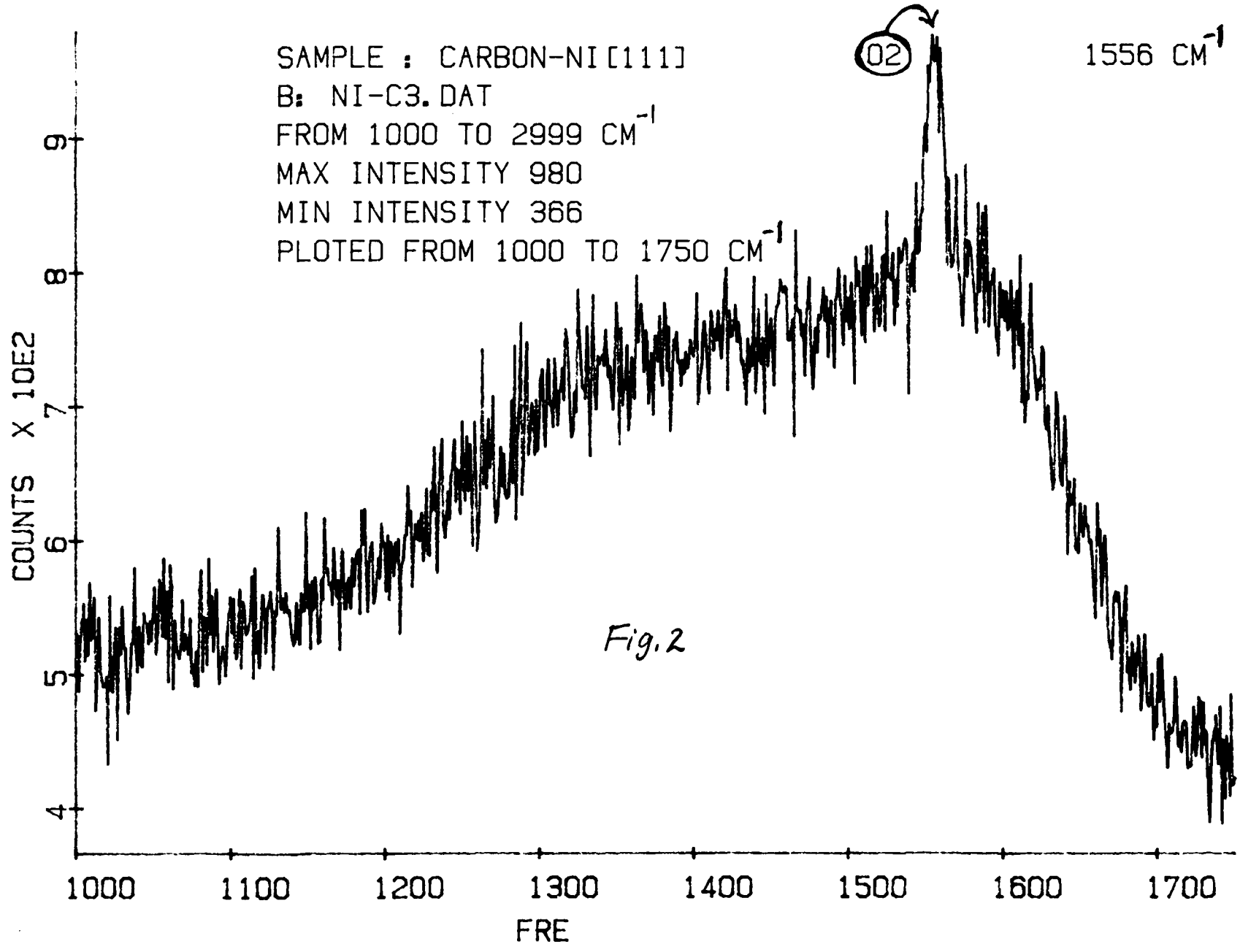

Fig. 2

LASER: 200 MW @ 488 NM. SLITS: 20 MIC. DATE 12-9-87
1 SCAN(S). TIME: 1 SEC/PT. PTS SPACED BY 1 FRE

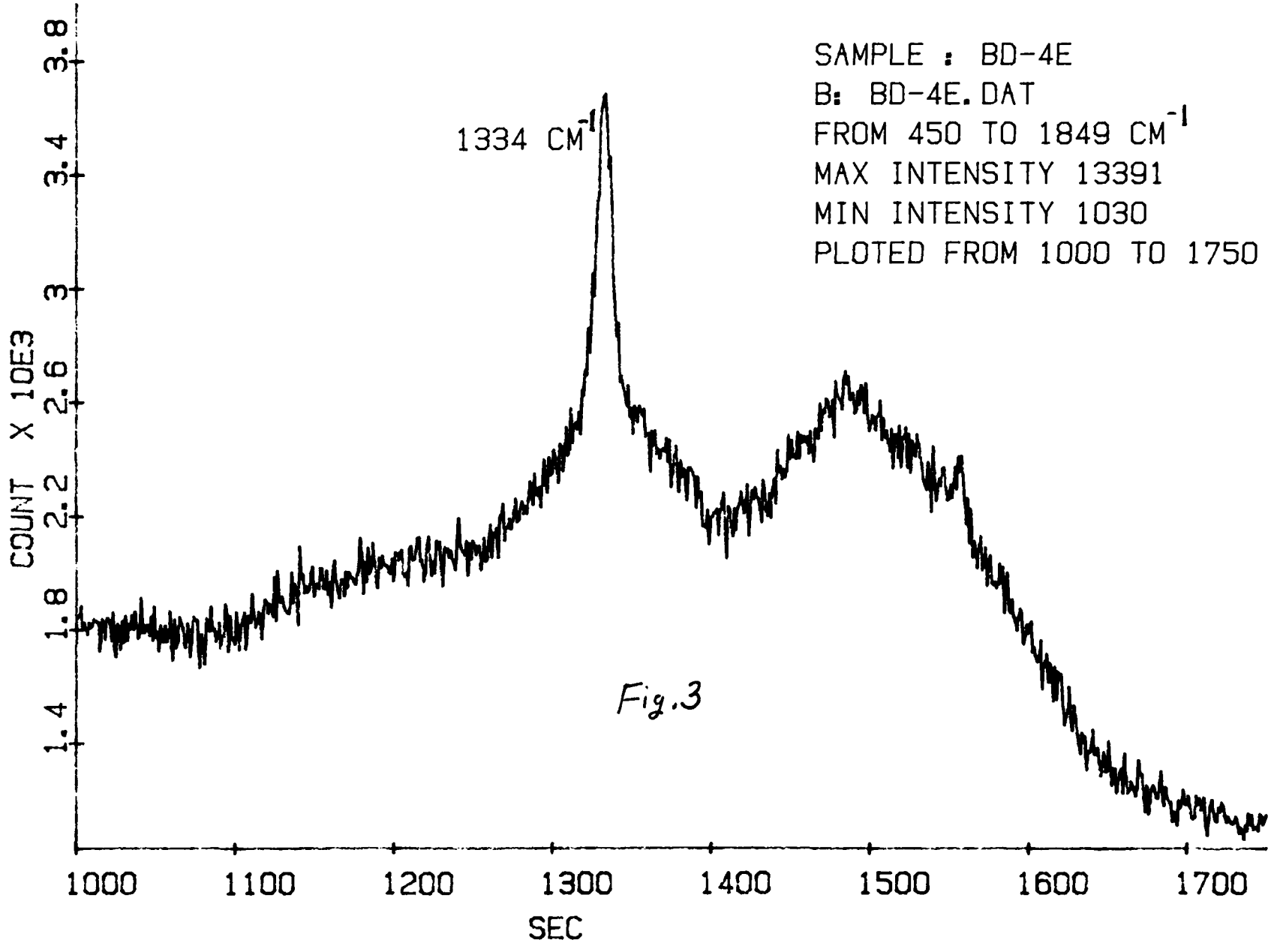

Fig.3

LASER: 200 MW @ 514.5 NM. SLITS: 10 MIC. DATE 10-28-87
1 SCAN(S). TIME: 1 SEC/PT. PTS SPACED BY 1 SEC

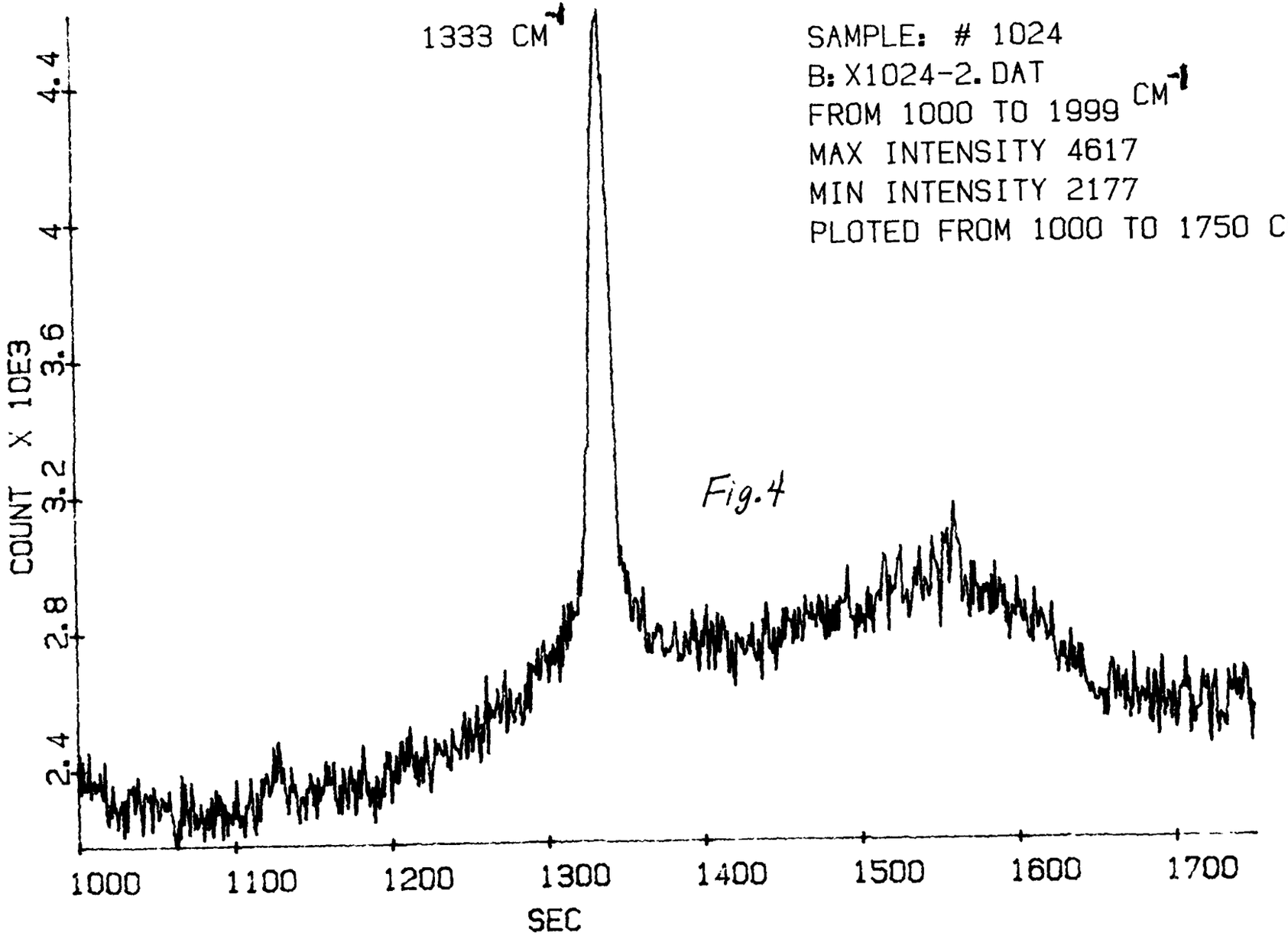
1333 CM-1
SAMPLE: # 1024
B: X1024-2.DAT
FROM 1000 TO 1999 CM-1
MAX INTENSITY 4617
MIN INTENSITY 2177
PLOTED FROM 1000 TO 1750 CM-1
COUNT X 10E3
4.4
4
3.6
3.2
2.8
2.4
1000
1100
1200
1300
1400
1500
1600
1700
SEC
LASER: 500 MW @ 514.5 NM. SLITS: 20 MIC. DATE 3-17-88
1 SCAN(S), TIME: 1 SEC/PT, PTS SPACED BY 1 SEC

Fig.4

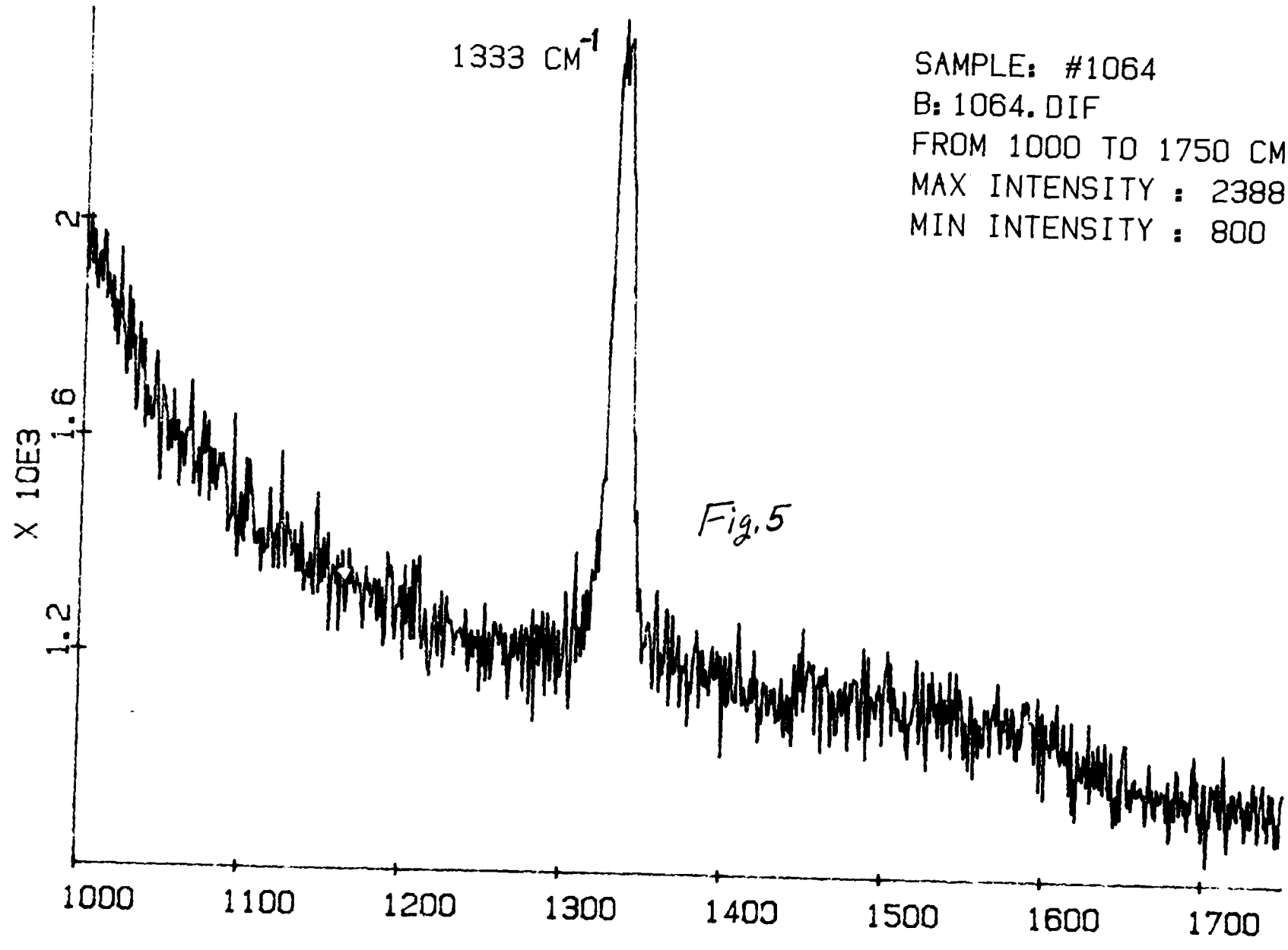
1333 CM-1
SAMPLE: #1064
B: 1064.DIF
FROM 1000 TO 1750 CM-1
MAX INTENSITY : 2388
MIN INTENSITY : 800
X 10E3
2
1.6
1.2
1000
1100
1200
1300
1400
1500
1600
1700
LASER: 0 MW @ 0 NM. SLITS: 0 MIC. DATE
0 SCAN(S), TIME: 0 SEC/PT. PTS SPACED BY 1

Fig. 5

B. Raman spectra from bulk crystalline diamond and from crystalline graphite.

A Raman spectrum from a 1/3 carat anvil-cut diamond is shown in Fig. 6. The very sharp 1330 cm^{-1} line (so intense that it is off scale) is diagnostic of crystalline diamond. Note that this sharp feature is totally absent in Figs. 1 and 2. In Fig. 6, the region from about 2000-2800 cm^{-1} contains the diamond overtone and/or other two or multi-phonon components. The sharp spike (*) is also diagnostic of crystalline diamond. This feature (*) is the overtone of the 1330 cm-1 line.

Raman spectra from crystalline graphite are shown in Figs. 7(a) and 7(b). In both of these figures, the line due to molecular O_2 at about 1557 cm^{-1} has been removed by the computer. This line was <u>not</u> so removed in Fig. 2, where it gives rise to the sharp spike labelled O_2 in that figure. The peak frequency of the sharp graphite line is about 1583 cm^{-1}. Note that Figs. 1, 2, and 3 show contributions near 1583 cm^{-1}, whereas the contribution near 1583 cm^{-1} in Fig. 4 is weak, but still observable. However, it is shown subsequently that the 1583 cm^{-1} line is only diagnostic of the presence of graphite under special conditions, that is, only when other spectral features are absent.

C. Raman spectra from a wide range of amorphous carbons.

The broad 1350 cm^{-1} feature in Figs 1-3 occurs in all of the spectra that we have obtained from various amorphous carbons. (It also occurs in the Raman spectrum of glassy carbon, but there its intensity is <u>large</u>, relative to the 1600 cm^{-1} intensity, whereas in the spectra from amorphous carbons, just the opposite

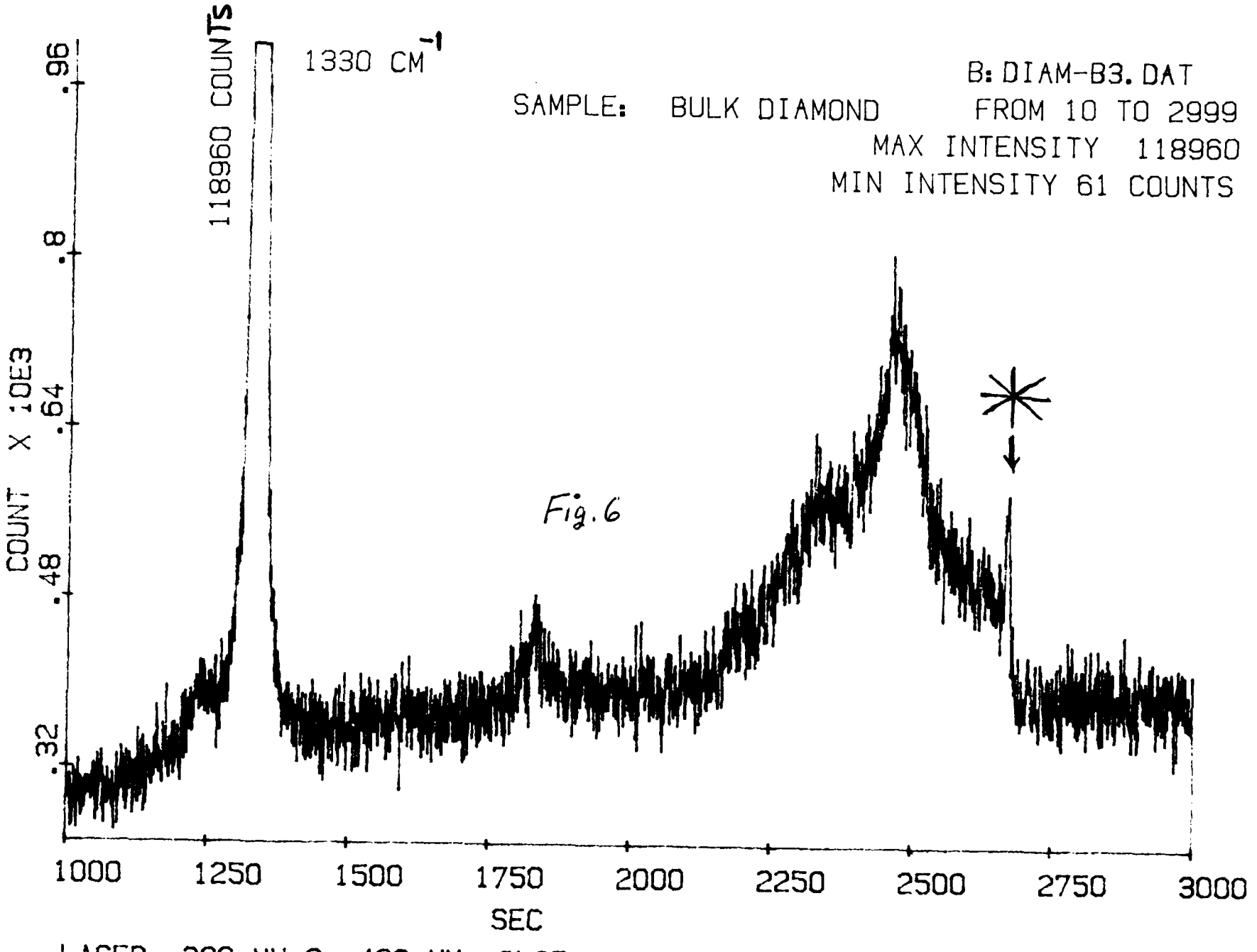

Fig. 6

LASER: 200 MW @ 488 NM. SLITS: 2 MIC. DATE 05-7-87
1 SCAN(S). TIME: .6 SEC/PT. PTS SPACED BY 1 SEC

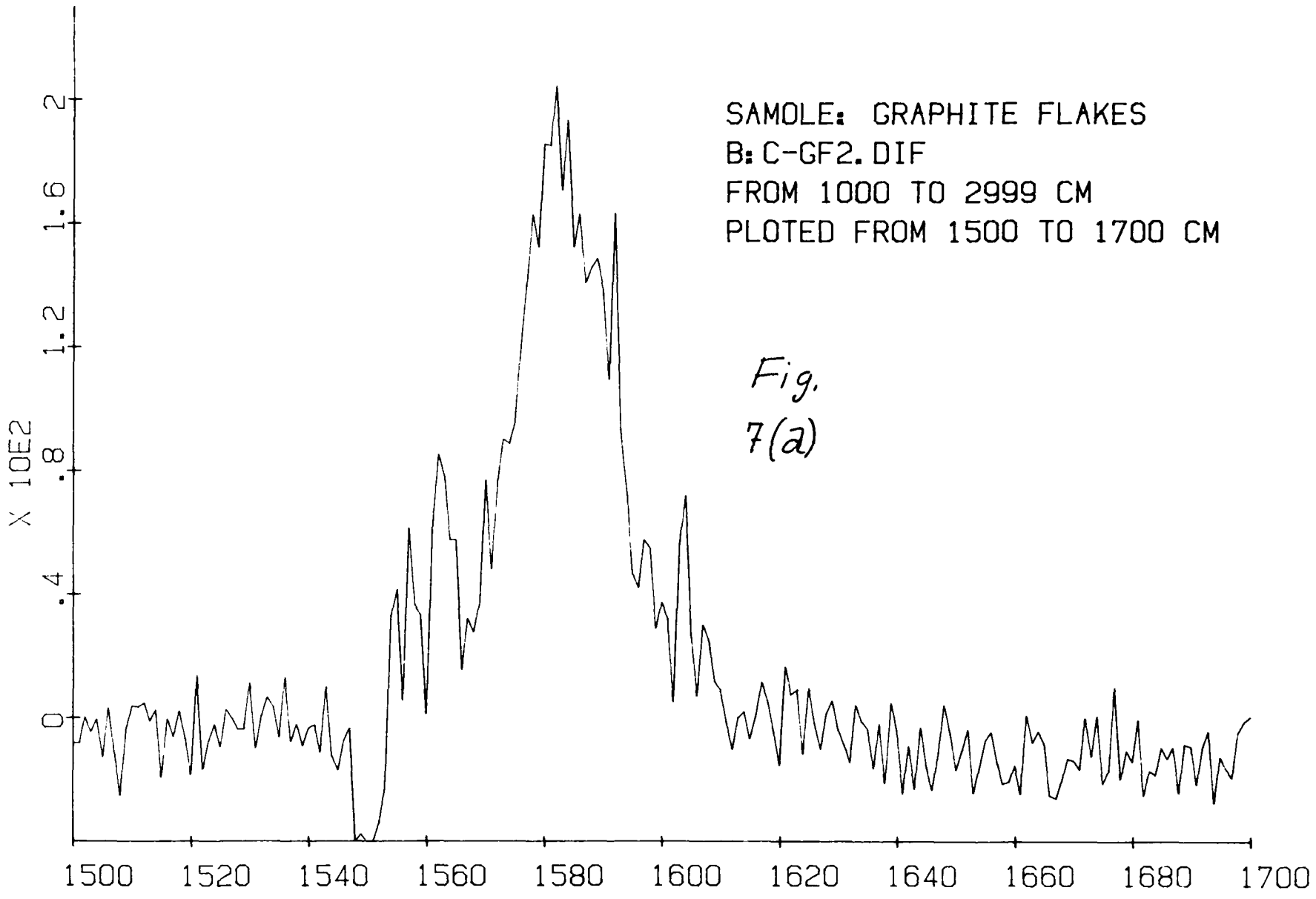

Fig. 7(a)

LASER: 0 MW @ 0 NM. SLITS: 0 MIC. DATE
0 SCAN(S), TIME: 0 SEC/PT, PTS SPACED BY 1

7(b)

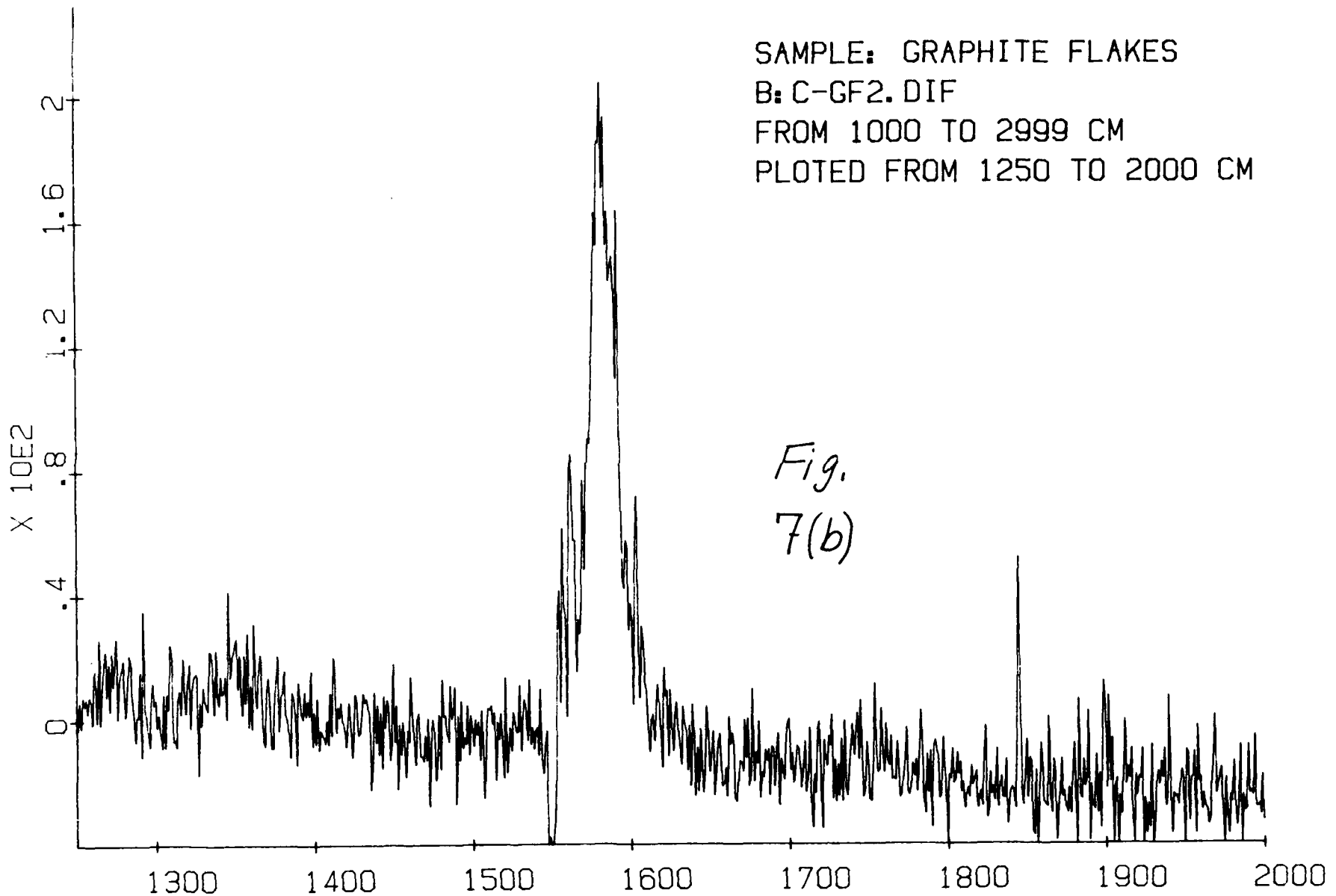
SAMPLE: GRAPHITE FLAKES
B: C-GF2.DIF
FROM 1000 TO 2999 CM
PLOTED FROM 1250 TO 2000 CM
X 10E2
0
.4
.8
1.2
1.6
2
1300
1400
1500
1600
1700
1800
1900
2000
LASER: 0 MW @ 0 NM. SLITS: 0 MIC. DATE
0 SCAN(S). TIME: 0 SEC/PT. PTS SPACED BY 1

Fig. 7(b)

intensity relationship occurs. Hence, we do not consider glassy or vitreous carbon in detail here.) The types of amorphous carbon that we have examined are as follows:

(α) lamp (or channel) black

(β) cocoanut shell charcoal

(Γ) carbon resulting from the acidic dissolution of spherulitic steel (cast iron).

(δ) carbon in Whetlerites (used in U. S. Army gas-masks).

(ε) chars (low-temperature, high-pressure aqueous digestion). These contain polycyclic aromatic hydrocarbons (PAH).

(Θ) soots (automobile). These are primarily PAH's.

(Ω) bone charcoal. These contain some phosphate.

Some, if not all, of the materials listed in (α) to (Ω) above, tend to burn to form CO_2 when excited by a laser beam in air. Therefore, we obtained the spectra in some cases by flooding the sample with Argon gas in the vicinity of the laser spot. Moreover, if we wished to keep the sample at room temperature, or if we wanted to study it below room temperature, we replaced the Argon gas with blow-off Nitrogen gas. When we did not use either Argon or Nitrogen, we observed Raman lines from air. The line from O_2 in air occurs near 1557 cm^{-1}, and the line from N_2 in air occurs near 2328 cm^{-1}. These lines could be, and were removed, in some cases by the computer. However, these two unwanted lines are so sharp, that they are immediately recognized, and thus they were not removed in all cases.

Raman spectra corresponding to (α) to (Ω), i.e., the

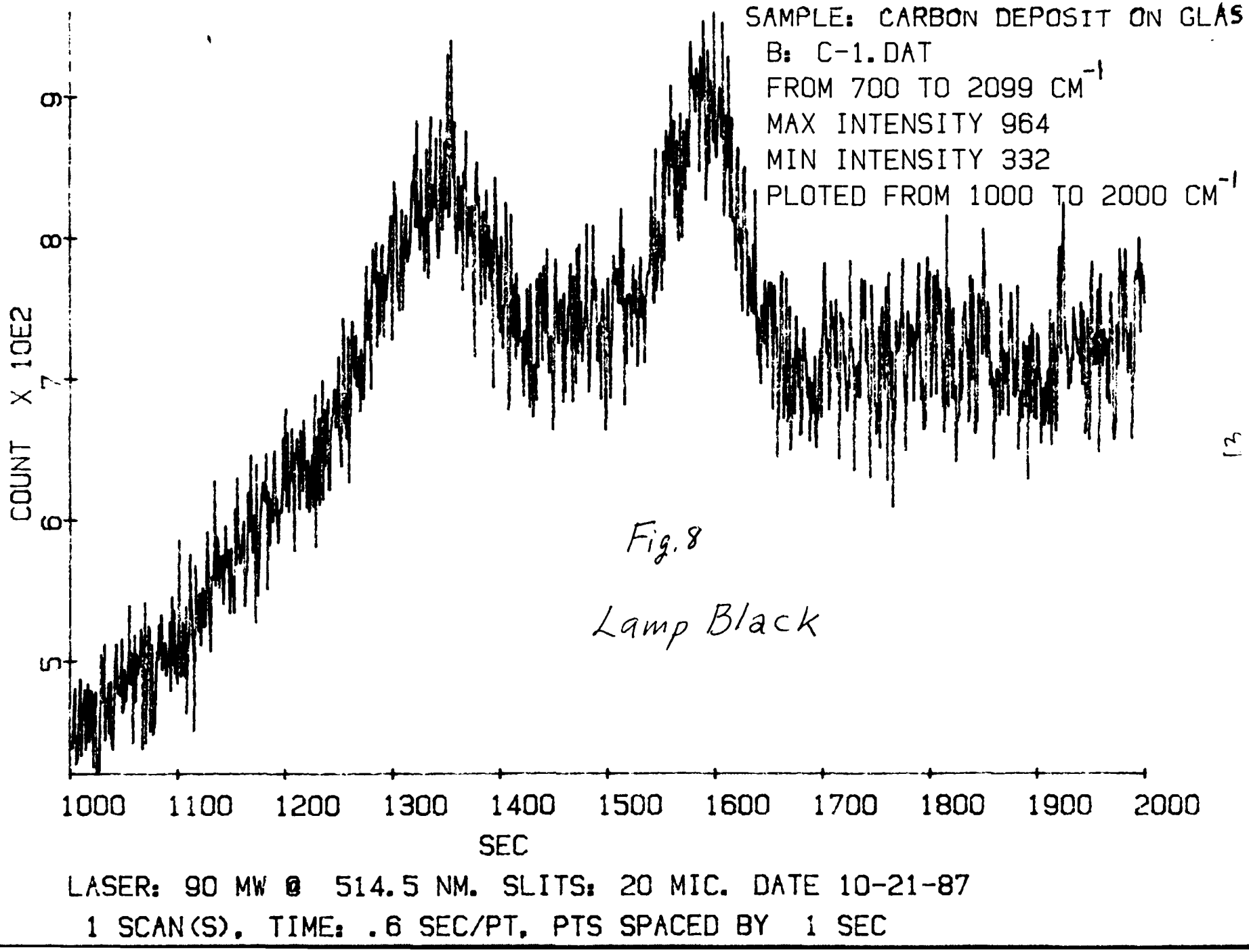

Fig. 8

Lamp Black

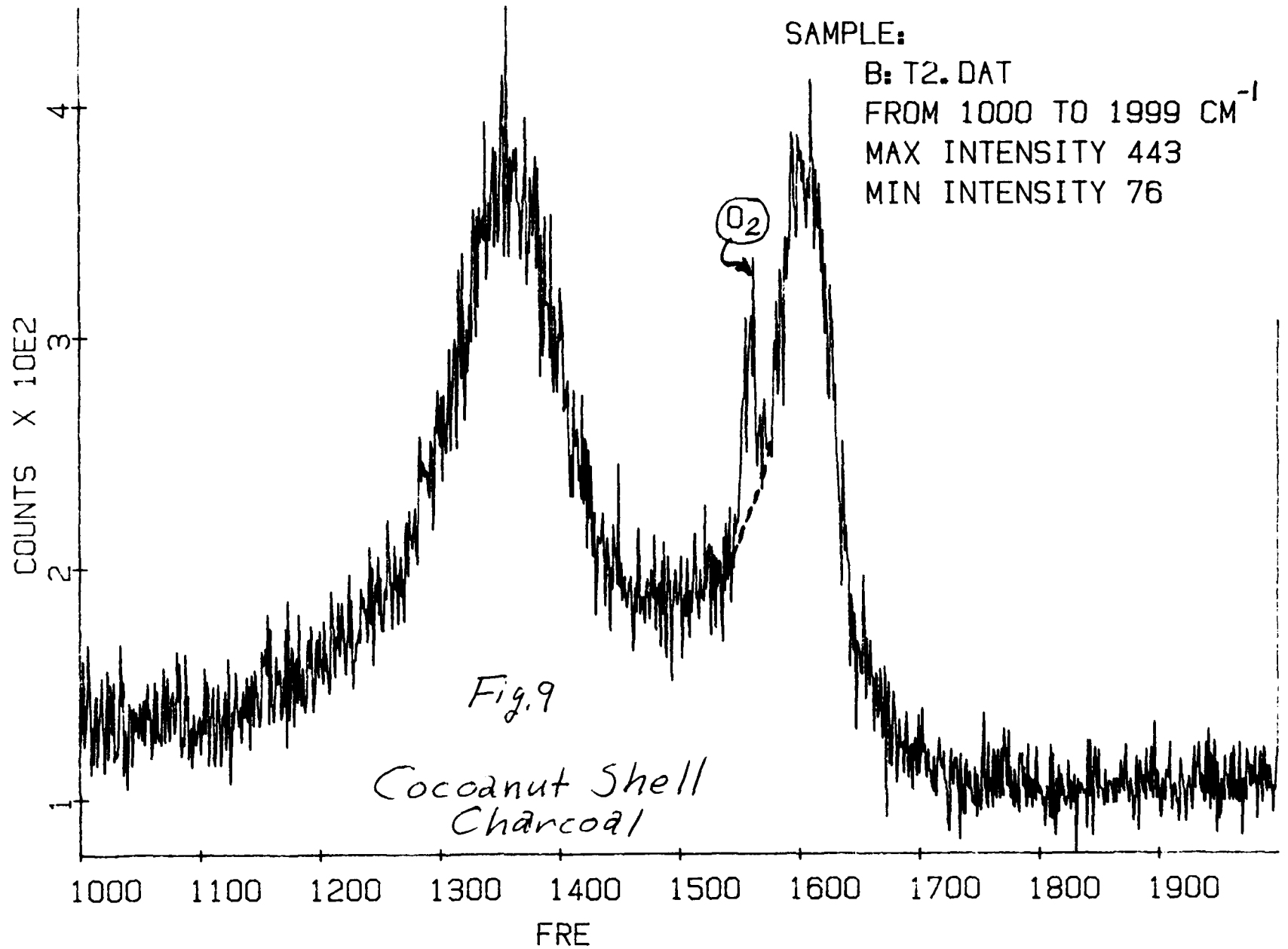
SAMPLE:
B: T2.DAT
FROM 1000 TO 1999 CM-1
MAX INTENSITY 443
MIN INTENSITY 76
O2
COUNTS X 10E2
1
2
3
4
1000
1100
1200
1300
1400
1500
1600
1700
1800
1900
FRE
Fig.9
Cocoanut Shell
Charcoal
LASER: 200 MW @ 488 NM. SLITS: 20 MIC. DATE 11-19-87
1 SCAN(S). TIME: 1 SEC/PT. PTS SPACED BY 1 FRE

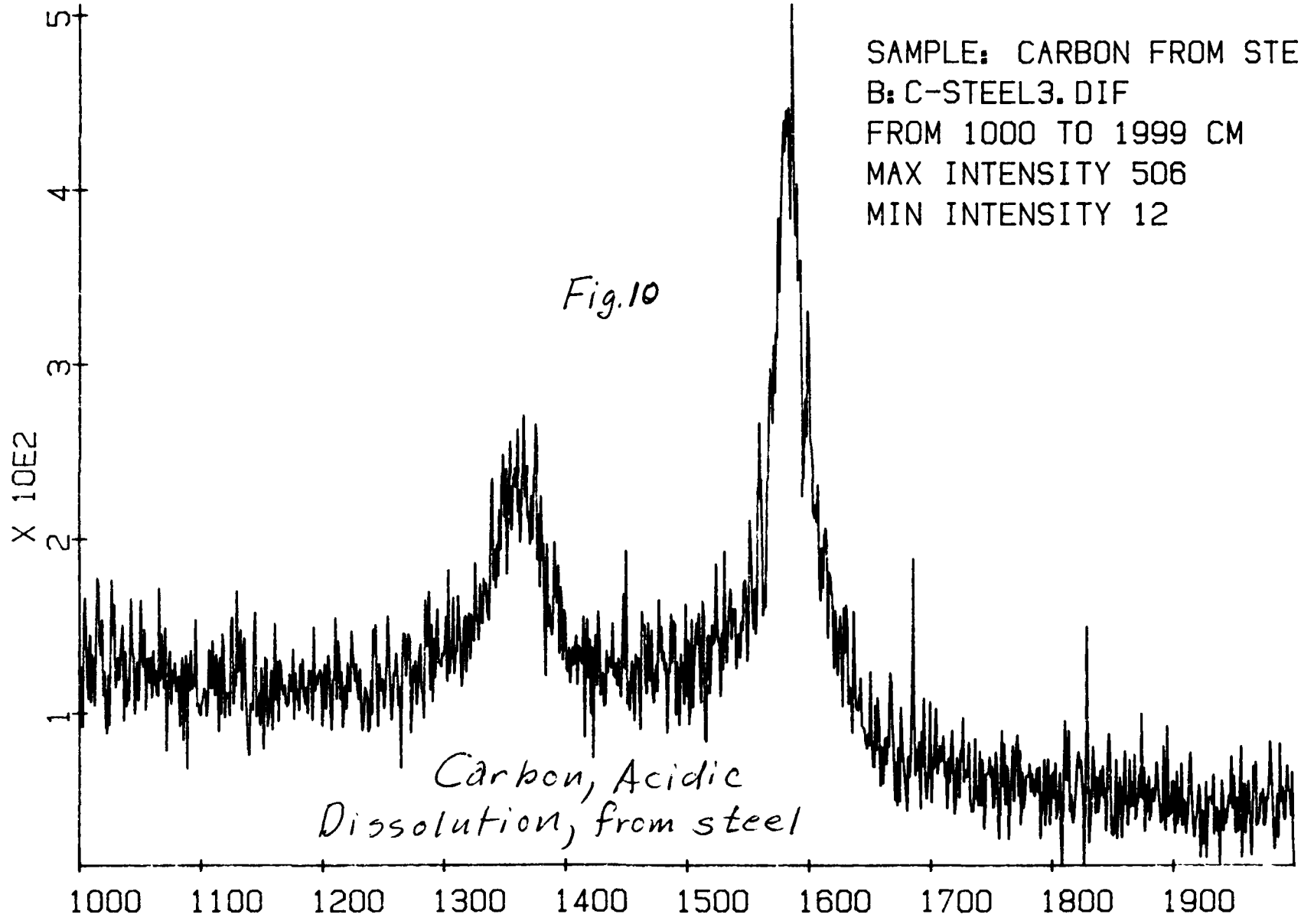

Fig.10

LASER: 0 MW @ 0 NM. SLITS: 0 MIC. DATE
0 SCAN(S). TIME: 0 SEC/PT. PTS SPACED BY 1

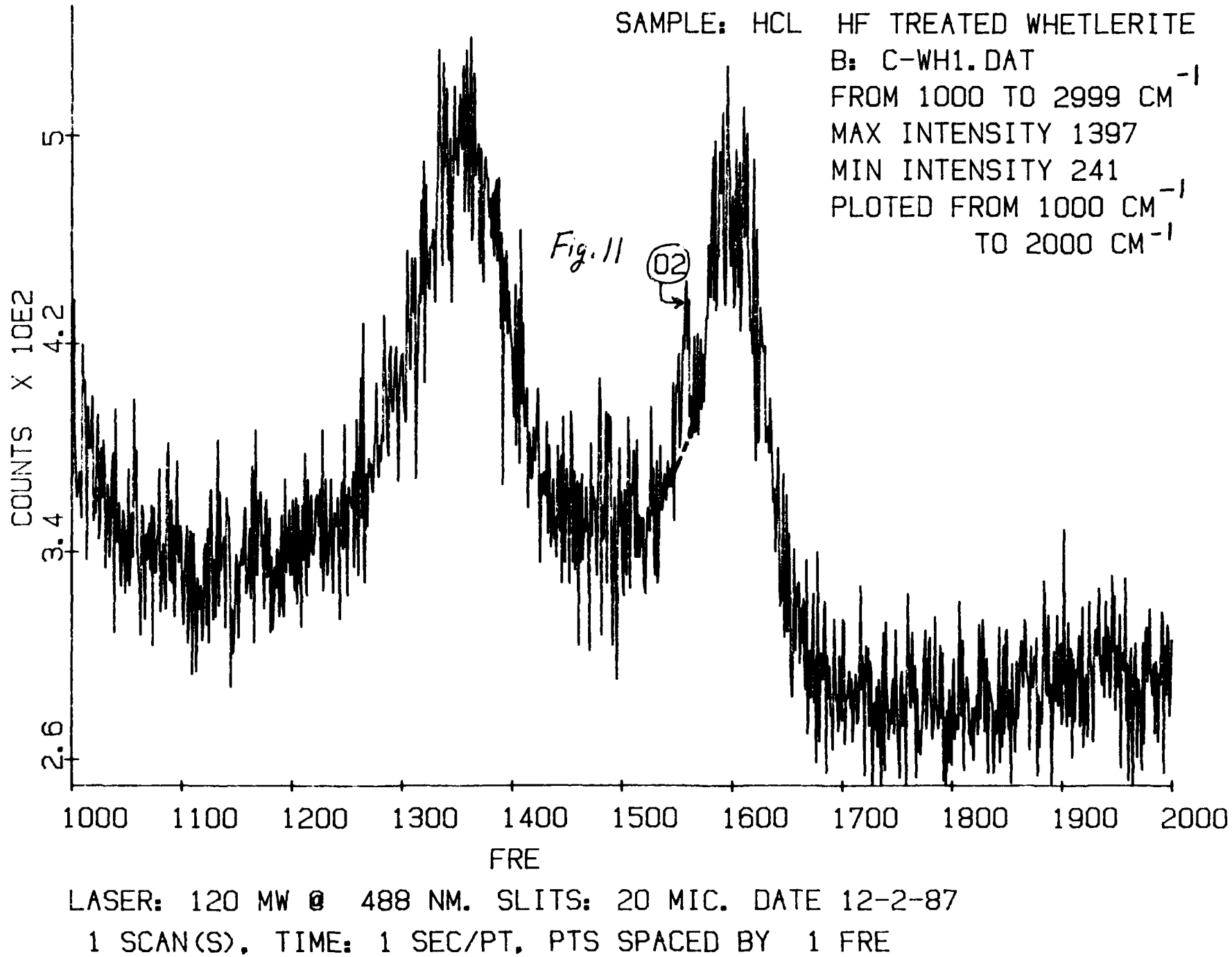
SAMPLE: HCL HF TREATED WHETLERITE
B: C-WH1.DAT
FROM 1000 TO 2999 CM-1
MAX INTENSITY 1397
MIN INTENSITY 241
PLOTED FROM 1000 CM-1
TO 2000 CM-1
Fig. 11
02
COUNTS X 10E2
5
4.2
3.4
2.6
1000
1100
1200
1300
1400
1500
1600
1700
1800
1900
2000
FRE
LASER: 120 MW @ 488 NM. SLITS: 20 MIC. DATE 12-2-87
1 SCAN(S), TIME: 1 SEC/PT, PTS SPACED BY 1 FRE

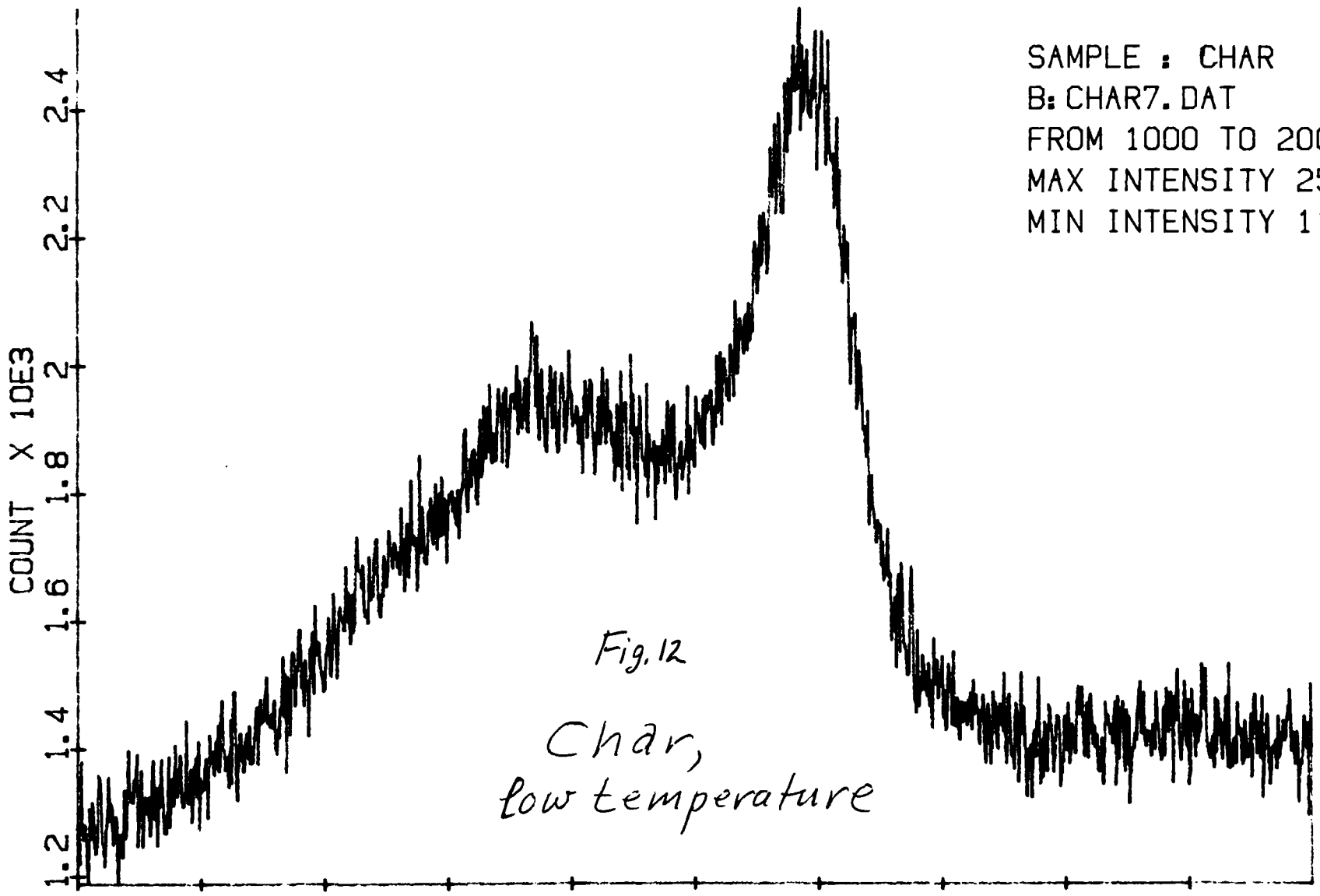

Fig. 12

Char, low temperature

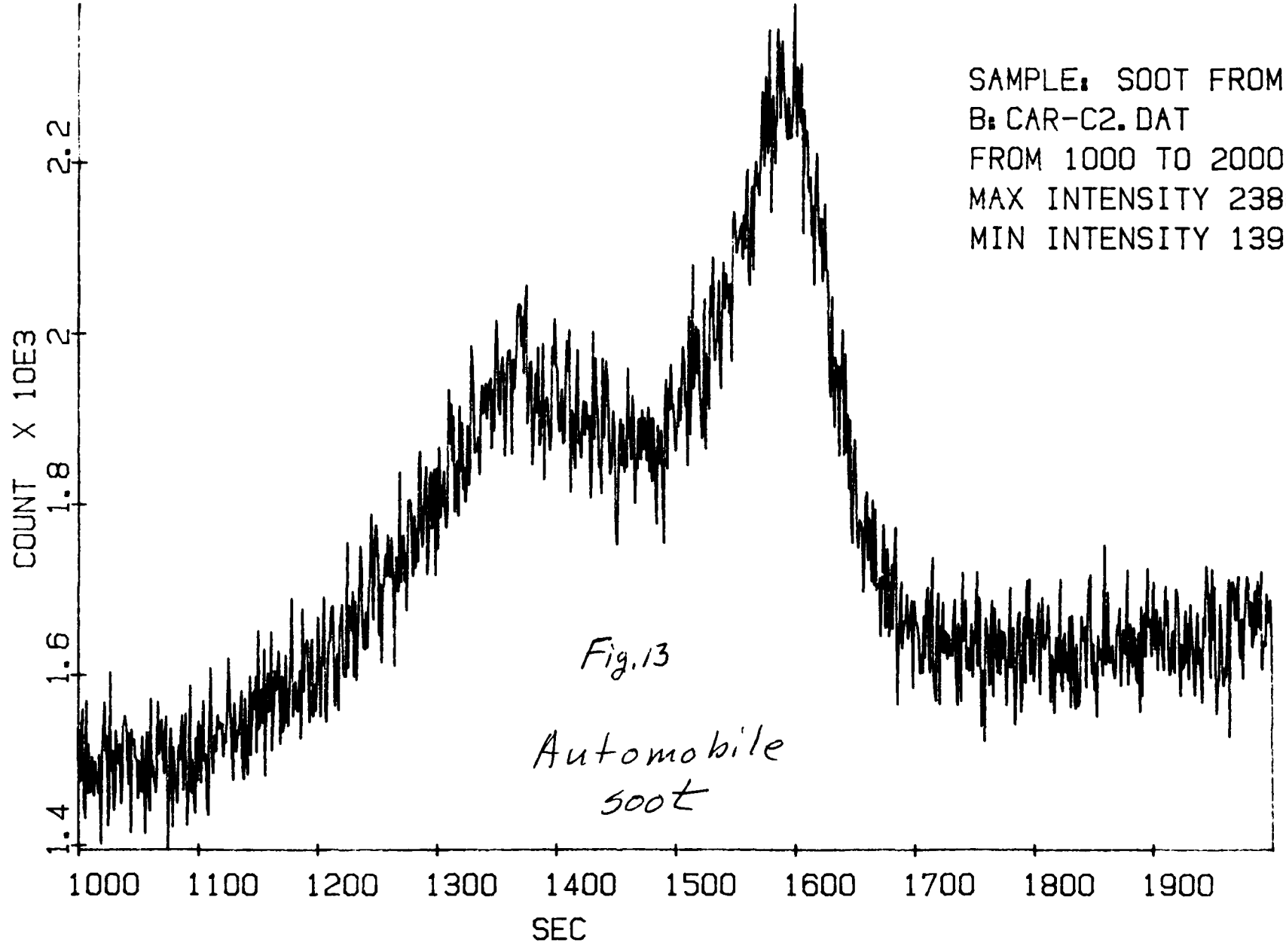
SAMPLE: SOOT FROM CAR
B: CAR-C2.DAT
FROM 1000 TO 2000 CM-1
MAX INTENSITY 2386
MIN INTENSITY 1395
COUNT X 10E3
2.2
2
1.8
1.6
1.4
1000
1100
1200
1300
1400
1500
1600
1700
1800
1900
SEC
Fig.13
Automobile soot
LASER: 120 MW @ 488 NM. SLITS: 20 MIC. DATE 05-31-88
1 SCAN(S), TIME: 1 SEC/PT, PTS SPACED BY 1 SEC

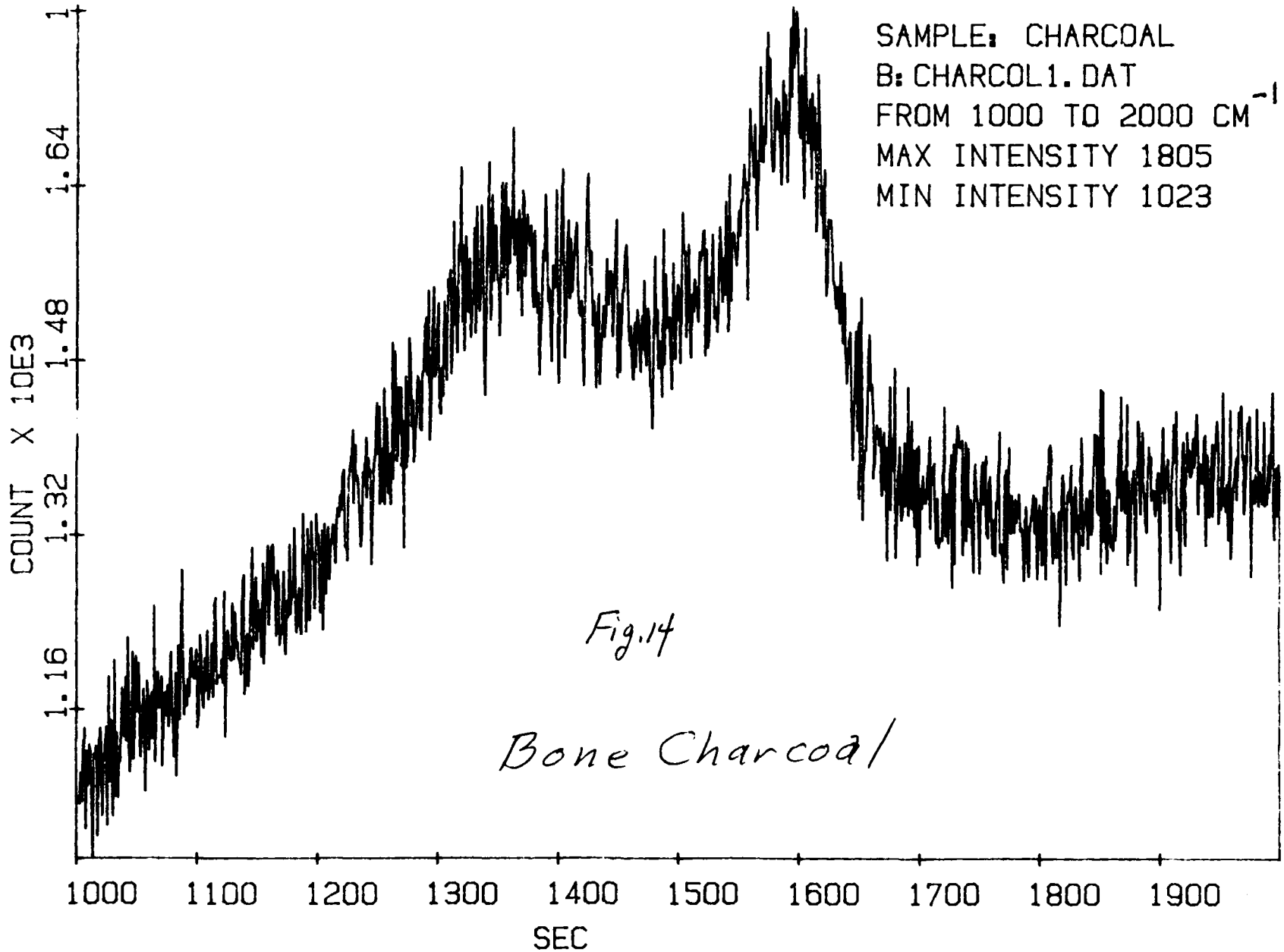
SAMPLE: CHARCOAL
B: CHARCOL1.DAT
FROM 1000 TO 2000 CM-1
MAX INTENSITY 1805
MIN INTENSITY 1023
COUNT X 10E3
1
1.64
1.48
1.32
1.16
1000
1100
1200
1300
1400
1500
1600
1700
1800
1900
SEC
Fig.14
Bone Charcoal
LASER: 120 MW @ 514.5 NM. SLITS: 20 MIC. DATE 05-27-88
1 SCAN(S). TIME: 1 SEC/PT. PTS SPACED BY 1 SEC

7 types of amorphous samples listed above, are shown in Figs. 8 to 14.

All Raman spectra shown in Figs. 8 to 14 display peaks near (nominally) 1350 cm^{-1} and near (nominally) 1600 cm^{-1}. Variations in intensity, and in half-width occur, however. In this report we will emphasize the sizeable variations in half-width (full-width at half-height, FWHH) that we have observed. Specifically, we will discuss the ratio of the FWHH's of two bands, which we give the symbol, R_w. R_w is the ratio of the FWHH of the nominal 1350 cm^{-1} band, to the FWHH of the nominal 1600 cm^{-1} band.

Before considering R_w values in detail, the reader should examine Fig. 12. Here, the 1350 cm^{-1} band is visually very broad compared to the 1600 cm^{-1} band. Next, examine Fig. 11. Here, the 1350 cm^{-1} band is not so broad, compared to the 1600 cm^{-1} band. It is this situation which we will be considering in a more quantitative fashion by measurements of the R_w ratio. Moreover, the importance of the R_w value becomes particularly evident when it is realized that this ratio is only about 0.8 or 0.9 for diamond films, compared to about 3.7 for chars. In other words, R_w decreases by about a factor of 5 in going from chars to diamond films.

Values of the ratio R_w are tabulated in Table I.

All of the entries in Table I refer to amorphous forms of carbon, that is, these carbons would not show x-ray diffraction. Nevertheless, the corresponding Raman spectra all vary. Obviously, a broad range of microscopic structures exists even

TABLE I

R_w = FWHH(≈1350)/FWHH(≈1580-1600)

SAMPLE	RATIO, R_w
CHAR	3.7
AUTO SOOT	2.3[5]
BONE CHARCOAL	1.9[5]
CARBON FROM SPHERULITIC STEEL	1.9
COCOANUT SHELL CHARCOAL	1.8
LAMP BLACK	1.7
WHETLERITE	1.7
THICK (MICRONS) DIAMOND FILM	0.8 - 0.9

for amorphous carbons. Or, stated alternatively, when one uses the term "amorphous", one is making a negative statement, that is, one is stating that the material lacks long range order. But the Raman data, on the other hand, are sensitive to local order. And, this local order can vary markedly in the absence of long range order. An understanding of the local order may be very important in relation to the conditions necessary for the optimum growth of diamond films, as indicated below.

3. Interpretation.

A. The sharp 1330 cm^{-1} Raman line and the ca. 1600 cm^{-1} line.

The sharp 1330 cm^{-1} feature from diamond and the 1583 cm^{-1} feature from graphite have been studied extensively. The 1330 cm^{-1} line is diagnostic of the presence of crystalline diamond. However, polycyclic aromatic hydrocarbons (which can be the precursors of diamond and graphite formation in some cases) can yield a line near 1583 cm^{-1} along with a broad 1350 cm^{-1} line. Hence, the 1583 cm^{-1} feature is not necessarily diagnostic of the presence of graphite, when the 1350 cm^{-1} feature is present, as in the case of diamond films. Other factors, such as narrowness, intensity, nature of the overtone spectrum, etc., are required to determined the presence of graphite unequivocally.

B. Width (FWHH) of the 1350 cm^{-1} feature; relation to diamond growth.

To our knowledge, the broad 1350 cm^{-1} feature has not yet been unequivocally assigned. Glassy or vitreous carbon is known to produce Raman features near 1580 and 1350 cm^{-1}, but the order

of the intensities of these two features is inverted from that seen here for amorphous carbons, as well as for diamond films, see Fig. 2 or 3. Hence, we feel that is would be grossly premature to relate the 1350 cm^{-1} feature from diamond films to glassy (vitreous) carbon. Moreover, the further question of the microscopic nature of the vibrations involved would not be resolved, even if such a premature assignment were made.

In the following discussion, we will describe some of the processes and temperatures involved in the pyrolysis of various organic precursors that can lead to the eventual formation of graphite. We emphasize that many of these processes are <u>not</u> those that are involved in the formation of diamond films. However, there are some features which are common to the eventual formation of graphite regardless of path, that is, these features are independent of the method of synthesis. Moreover, we describe the pyrolytic processes, because we can relate some features of these pyrolytic processes to the R_w values which we have measured. And, from the understanding that is gained, we can make some inferences which we believe are pertinent to diamond film formation.

When the organic precursors (of graphite) are subjected to pyrolysis a sequence of structures occurs which depends primarily upon the temperatures attained. These pyrolytic processes are now fairly well understood, and may be described in 4 stages as follows:

Stage A. When the temperature of the pyrolysis of an organic precursor, e.g., pitch, wood, natural fibers, etc., is

held below about 1000 °C, polycyclic aromatic hydrocarbons are formed involving condensed ring systems of 10 rings or less. An example of a condensed ring system is CORONENE. Coronene is a condensed aromatic ring system involving six rings. Its formula is $C_{24}H_{12}$. Its ring system is reminiscent of graphite, except for its H atoms. Circobiphenyl is a system of 10 rings, and its formula is $C_{38}H_{20}$. It would be about the biggest ring system that might occur in Stage A. Stage A would involve single C-C bonds, double C=C bonds, and C-H bonds. Stage A would also involve other atoms such as O, N, S, etc., but these would be lost at higher temperatures, i.e., in Stage B, etc.

Stage B. Stage B would involve further pyrolysis that occurs at temperatures up to roughly 1600 °C. In this stage a reasonable amount of stacking-up of the polycyclic ring systems would occur. That is, the planar polycyclic ring systems would tend to stack-up to form some columnar type structures. Many of the non-carbonaceous materials would go off in this stage, for example, as NH_3, SO_2, H_2O, etc. The columnar structures would not be completely regular, however. Faults, dislocations, sp^3 carbon sites, etc., would abound. And it is this stage which we believe would be favorable for the eventual formation of diamond, because of the sp^3 carbon atoms, and because graphite has not yet begun to form, and to compete against diamond.

Stage C. In this stage temperatures to about 2000 °C are involved. Here, wrinkled graphitic structures are formed.

Stage D. In this stage temperatures of 2000 °C and above are involved. These temperatures lead to the formation of

graphite.

We have obtained Raman spectra from amorphous carbons which encompass the lower part of the temperature range ultimately leading to graphite. Moreover, it appears to us that the Rw values decline, at least qualitatively, as the temperature of the pyrolysis rises.

The char of Table I has an Rw value of 3.7. This char was formed by treatment of an aqueous slurry at 250-265 °C and under a pressure of 2000-4000 psi.

The Whetlerite of Table I was formed in two stages. The temperature of the final stage was 900-1000 °C. Here the Rw value has decreased to 1.7. (We regard values of 1.7 to 1.95 in Table I to be essentially the same within present experimental error.)

Finally, the diamond film, Table I, has an Rw value of about 0.8 or 0.9. This suggests that the diamond film has been formed at "effective" temperatures in excess of 1000 °C. In this regard it should be noted that rotational temperatures, for example, of excited fragments in a plasma can exceed the thermodynamic temperature.

In stage B where stacking predominates, one would expect numerous terminal C-H groups, dislocations, defects, and sp^3 bonding of the carbon. In stages C or D, on the other hand, the system has either formed graphitic layers, or is well on the way to forming such layers. Obviously, the chance that true crystalline diamond can form is greatly diminished in stages C and D. The best chance of forming crystalline diamond would seem

to involve stage B, where sp^3 bonding is prevalent, and where such bonding would lead to the 3-dimensional diamond structure.

In regard to diamond formation, we know of no diamond film that shows only the pure crystalline diamond spectrum, plus the pure graphite spectrum. In our experience diamond films show both of the 1350 and 1600 cm^{-1} features when crystalline diamond is absent. But, even when the crystalline diamond peak at 1330 cm^{-1} is extremely intense, traces of both of the 1350 and 1600 cm^{-1} features remain. This indicates that true graphite was never formed, and because this thermodynamically stable state was never reached, it never competed with diamond formation.

Evidence for the presence of the 1350 and 1600 cm^{-1} features when the 1330 cm^{-1} crystalline diamond line is extremely strong is present in Figs. 4 and 5. For example, in Fig. 5, if an upwardly concave baseline is drawn from about 1300 to 1800 cm^{-1}, it is evident that the broad 1350 cm^{-1} feature is still present underneath the sharp 1330 cm^{-1} crystalline diamond line. The same conclusion is even more readily obtained from Fig. 4.

Before making a tentative assignment of the Raman lines seen for diamond films, with and without crystalline diamond, it is useful to consider some general assignments or group frequencies.

It is well known from the vibrational spectroscopy of organic materials which contain conjugated C=C double bonds that the out-of-phase C=C vibrations occur near 1590 cm^{-1} and that the in-phase C=C vibrations occur near 1610-1640 cm^{-1}. Moreover, the Raman line from benzene near 1600 cm^{-1} is one of the strongest lines in the spectrum. Clearly, the 1583 cm^{-1} frequency from

graphite corresponds to vibrations of the C=C double bonds. However, polycyclic aromatic hydrocarbons also produce vibrational frequencies near 1583 cm^{-1}, and thus it is not necessary to invoke the presence of graphite to explain the Raman spectra from diamond films. Moreover, splittings observed from the diamond films in the vicinity of roughly 1600 cm^{-1} may be the result of in-phase and out-of-phase Raman vibrations of polycyclic aromatic hydrocarbons, etc., which are both allowed due to various perturbations, e.g., selection rule violations.

The broad 1350 cm^{-1} feature observed here from diamond films and from amorphous carbons is more difficult to assign, but the best example of a vibrational frequency near 1350 cm^{-1} is the 1330 cm^{-1} line from diamond itself. Because diamond involves a 3-dimentional lattice and sp^3 bonding, it seems reasonable to assume that the broad 1350 cm^{-1} feature arises from sp^3 bonding in which a range of bond angles and distances is involved. This range of angles and distances would give rise to a range of force constants for the C-C vibrations which, in turn, would give rise to the observed broadening.

Of course, other types of vibrations occur near 1350 cm^{-1}. In plane C-H deformation vibrations occur in the general vicinity of 1330 cm^{-1}. Fulvenes show an intense vibration near 1340-1370 cm^{-1} which is not related to CH_3 deformation, but rather is characteristic of unsaturated five-member rings. This vibration is also seen from indene and cyclopentadiene. Coronene also displays an intense vibration near 1320 cm^{-1}. Hence, in a complex mixture of polycyclic aromatic hydrocarbons, one could

expect to observe many vibrations near 1350 cm^{-1}.

We feel nevertheless, that while C-H deformations and other types of vibrations might add to the breadth and complexity of the 1350 cm^{-1} contour, that the main contributions to that contour arise from sp^3 carbon bonding. We also feel that the main contribution to the breadth of the 1350 cm^{-1} contour arises from inhomogeneous broadening effects, that is, from a range of bond angles and bond distances, primarily the latter. Hence, it is our hypothesis that the width of the 1350 cm^{-1} contour is a measure of the randomness of the structures engaged in sp^3 bonding, which in turn explains why this randomness decreases with rising temperature.

In other words, increase of temperature in terms of the polycyclic aromatic hydrocarbon model discussed previously, moves the system from a random array of relatively small (10-membered) ring systems, to a stacking-up of larger ring systems, albeit an imperfect stacking, to a stacking of wrinkled graphite layers, and finally to the well-ordered stacking of parallel planes, to yield the ultimate, thermodynamically stable phase, crystalline graphite.

One further comment about the polycyclic aromatic hydrocarbon model should also be made. There has been much discussion about the mechanism of diamond formation from the vapor phase, and the idea that sp^3 bonding is initiated from CH_3 groups has been advanced. However, there seems to be at least some agreement amoung astrophysicists that large polycyclic aromatic hydrocarbons can be produced from condensation of CH_4 in space.

That is, when ionizing radiation, or circumstances which produce plasmas are present, condensation reactions occur which lead to polycyclic aromatic hydrocarbons. Hence, one cannot rule out condensation type reactions in the plasma or hot wire methods of producing diamond films. Furthermore, the polycyclic aromatic hydrocarbon model is invoked almost universally to explain the production of amorphous carbons.

Finally, we have noticed that when a large amount of crystalline diamond is present in the diamond film, that the broad Raman peak nominally at about 1600 cm^{-1} shifts downward, reaching values as low as about 1485 cm^{-1}. Under these conditions the broad 1350 cm^{-1} feature is still present, however, and it will be necessary to deconvolute this peak from the overall contour of the two peaks to determine the exact frequency of the nominal 1600 cm^{-1} feature. We do not understand this effect, and expect to examine it further. It may be in the direction of decreasing the double-bond force constant, which in turn would suggest that the double-bond distances are lengthening. It could also be related to cross-linking or inter-planar bonding.

Annual Technical Reports Distribution List

SDIO/IST Crystalline Carbon Materials Program

(to be incorporated into report as its final pages)

addressee	quantity
1. ONR Arlington, VA 22217 ATTN: Code 1114	8
Code 1131M	1
2. Defense Documentation Center Bldg. 5 Cameron Station Alexandria, VA 22314	12
3. Naval Research Laboratory Washington, DC 20375 ATTN: Code 4683	1
Code 2627	6
Code 6820	1
Code 6211	1
Code 6684	1
Code 6115	1
Code 4684	1
4. Naval Ocean Systems Center San Diego, CA 92152 ATTN: Code 1211	1
Code 911	1
Code 56	1
5. (Cognizant ONR Resident Representative or DCASMR)	1
6. SDIO/IST Pentagon Washington, DC 20301-7100	1
7. DARPA/D.S.O. 1400 Wilson Blvd. Arlington, VA 22209	1
8. Dr. M. Geis M.I.T. Lincoln Labs Lexington, MA 02173-0073	1
9. Prof. R. Messier 265 Materials Res. Lab. University Park, PA 16802	1
10. Prof. R. Davis Materials Eng., N.C.S.U. Raleigh, NC 27695-7907	1
11. R. Markunas R.T. Instit., P.O. Box 12194 R.T. Park, NC 27709-2194	1
12. Prof. G. Walrafen Howard Univ., Chemistry Dept. 5325 Potomac Ave., N.W. Washington, DC 20016	1
13. Prof. I. Lindau Synchrotron Radiation Lab. Stanford, CA 94305	1
14. A. J. Purdes M.S. 147 Texas Instruments, P.O. Box 655936 Dallas, TX 75265	1
15. W. D. Partlow Westinghouse R&D Ctr. 1310 Beulah Road Pittsburgh, PA 15235	1
16. R. L. Adams 21002 N. 19th Ave., Suite 5 Phoenix, AZ 85027	1

Annual Technical Reports Distribution List

SDIO/IST Crystalline Carbon Materials Program

(to be incorporated into report as its final pages)

addressee	quantity
17. Prof. J. Angus Dept. of Chemistry Case Western Reserve Univ. Cleveland, OH 44106	1
18. T.R. Anthony, GE R&D Bldg. K-1, Room 1C30 Schnectady, NY 12345	1
19. Yehuda Arie SRI Sarnoff Center Princeton, NJ 08540	1
20. P.J. Boudreaux, Lab for Phys. Sci. 4928 College Avenue College Park, MD 20740	1
21. Prof. R.F. Bunshaw, UCLA 6532 Buelter Hall Los Angeles, CA 90024	1
22. Ray Calloway, Aerospace Corp. P.O. Box 92957 Los Angeles, CA 90009	1
23. Prof. W.K. Chu, U.N.C. Phillips Hall 039-A Chapel Hill, NC 27517	1
24. IBM T.J. Watson Center Yorktown Heights, NY 1059 8 ATTN: J.J. Cuomo B. Meyerson	1 1
25. Prof. J. L. Davidson 200 Brown Hall Auburn Univ., AL 36849	1
26. Prof. P.H. Fang, Dept. of Physics Boston College Chestnut Hill, MA C2167	1
27. Wen Hsu, Div 8347 Box 969 Sandia National Labs Livermore, CA 94550	1
28. Prof. W. Lanford Physics Dept. S.U.N.Y. Albany, NY 12222	1
29. Prof. E.S. Machlin 44 Morningstar Drive Croton-on-Hudson, NY 10520	1
30. Prof. J. Mayer 210 Bard Hall Cornell University Ithaca, NY 14853	1
31. Prof. J. Pancove, ECE Univ. of Colorado Boulder, CO 80309-0425	1
32. Michael Pinneo, Crystallume 3180 Porter Drive, Suite 2 Palo Alto, CA 94304	1
33. Kenneth Russell J.P.L. M.S. 122-123 4800 Oak Grove Drive Pasadena, CA 91109	1
34. Prof. T. D. Moustakas Exxon Research Annandale, NJ 08801	1

Encl. (2)